Research Square

Preprints are preliminary reports that have not undergone peer review.
They should not be considered conclusive, used to inform clinical practice,
or referenced by the media as validated information.

# Calcium-enriched whey protein hydrolysate enhances calcium transport across Caco-2 monolayers: identification of calcium-binding peptides using a perfused intestine-on-chip

**Jessica Freire Feitor**

jessica.feitor@wyss.harvard.edu

Instituto de Química de São Carlos

**Ma Hui Ling**

Instituto de Química de São Carlos

**Laís Canniatti Brazaca**

Instituto de Química de São Carlos

**Vinícius Ferreira Guimarães**

Instituto de Química de São Carlos

**Sinara Teixeira Brasil Morais**

Instituto de Química de São Carlos

**Amanda Maciel Lima**

Instituto de Química de São Carlos

**Aline Teixeira Brasil Morais**

Instituto de Química de São Carlos

**Giulia Kassab**

Instituto de Física de São Carlos

**Emanuel Carrilho**

Instituto de Química de São Carlos

**Leif Horsfelt Skibsted**

University of Copenhagen

**Daniel Rodrigues Cardoso**

Instituto de Química de São Carlos

---

**Research Article**

**Keywords:** Intestine-on-chip, Calcium bioavailability, Caseinomacropeptide, Bioactive peptides, Caco-2, Whey protein hydrolysate

**Posted Date:** November 27th, 2026

**DOI:** https://doi.org/10.21203/rs.3.rs-11704428/v1

**License:** This work is licensed under a Creative Commons Attribution 4.0 International License.
Read Full License

**Additional Declarations:** No competing interests reported.

# Calcium-enriched whey protein hydrolysate enhances calcium transport across Caco-2 monolayers: identification of calcium-binding peptides using a perfused intestine-on-chip

Jéssica Freire Feitor[1,*], Ma Hui Ling[1,2], Laís Canniatti Brazaca[1,2], Vinícius Ferreira Guimarães[1,2], Sinara Teixeira Brasil Morais[1], Amanda Maciel Lima[1,2], Aline Teixeira Brasil Morais[1], Giulia Kassab[3], Emanuel Carrilho[1,2], Leif H. Skibsted[4], Daniel Rodrigues Cardoso[1,*]

[1]*Instituto de Química de São Carlos, Universidade de São Paulo, 13566-590 São Carlos, SP, Brazil*;

[2]*Instituto Nacional de Ciência e Tecnologia de Bioanalítica - INCTBio, 13083-970, Campinas, SP, Brazil;*

[3]*Instituto de Física de São Carlos, Universidade de São Paulo, 13566-590 São Carlos, SP, Brazil*.

[4]Department of Food Science, University of Copenhagen, DK-1958, Frederiksberg C, Denmark.

* Corresponding authors: drcardoso@usp.br and jessicafrefe@gmail.com

**Abstract:**

Calcium transport from food matrices may be influenced by the protein hydrolysates with which it is consumed. This study compared calcium transport from a commercial bovine whey protein hydrolysate, with and without calcium chloride enrichment, across Caco-2 monolayers cultured in commercial Transwell inserts and in two low-cost, perfused intestine-on-chip (IoC) devices: a single-use acrylic device and a reusable polydimethylsiloxane device. Calcium was quantified by electrospray ionization mass spectrometry following complexation with ethylenediaminetetraacetic acid, and transported peptides were examined by matrix-assisted laser desorption/ionization tandem mass spectrometry. In the static Transwell model, apparent calcium permeability from the hydrolysate was $10.2 \pm 1.0 \times 10^{-5}$ cm $s^{-1}$, compared with $3.8 \pm 1.7 \times 10^{-5}$ cm $s^{-1}$ for calcium chloride alone at the same calcium load. Perfused IoC culture supported confluent, tight-junction-positive monolayers by day 8, compared with day 21 in static Transwell culture, demonstrating faster establishment of the epithelial barrier. Two casein-derived peptide sequences were detected in transport samples, with calcium-associated ions providing candidates for further investigation. Together, these findings indicate greater apparent calcium permeability with hydrolysate in the Transwell model and demonstrate the potential of both perfused IoC devices for food-related transport studies.

**Keywords Intestine-on-chip, Calcium bioavailability, Caseinomacropeptide, Bioactive peptides, Caco-2, Whey protein hydrolysate**

# 1 Introduction

Organ-on-a-chip (OoC) systems combine living cells with microfluidic environments that can reproduce selected structural and dynamic features of human tissues in vitro [1-3]. By enabling controlled fluid flow and exposure conditions, these models provide tools for studying processes such as drug responses, toxicity, and nutrient transport [4, 5]. Their value depends, however, on the suitability of the model for the research question and on the ability to produce reliable, accessible devices.

Calcium is an essential dietary mineral, but its absorption depends not only on intake and physiological factors,including age, health status, vitamin D, and hormonal regulation, but also on interactions with other food components [6-10]. Dairy products are a major source of dietary calcium, making it important to understand how dairy ingredients and their processing affect calcium solubility and transport [8]. In vitro models can help investigate these interactions and compare potential strategies for improving calcium delivery, while avoiding the need to infer absorption from calcium content alone [9-13].

Intestine-on-a-chip (IoC) models have been used to study intestinal biology and drug or nutrient transport [14-19], but their application to food matrices remains limited [20-23]. Many experimental systems are static or require specialized fabrication and equipment, which can limit their accessibility for food-science research. More accessible perfused models could help researchers assess how food-derived ingredients interact with an intestinal epithelial barrier under controlled flow conditions. At the same time, device performance and reproducibility need to be evaluated against established cell-culture systems.

The present study assessed calcium transport from a commercial bovine whey protein hydrolysate (Peptigen®; Arla Foods Ingredients), with and without calcium enrichment, using

Caco-2 monolayers in conventional Transwell® inserts and two perfused IoC designs: a single-use acrylic device (SuA) and a reusable polydimethylsiloxane device (RPDMS). The devices were evaluated for fabrication, cell growth, and barrier formation, and their transport results were compared with those from Transwell® cultures. Calcium was quantified by direct-injection electrospray ionization mass spectrometry, while matrix-assisted laser desorption/ionization tandem mass spectrometry was used to examine peptides detected in transport samples and assess candidate calcium-peptide adducts. This study therefore combines a comparison of low-cost perfused culture devices with an investigation of calcium and peptide transport from a whey protein hydrolysate.

## 2 Materials and methods

### 2.1 Materials

Peptigen® IF3080 bovine whey protein hydrolysate was provided by Arla Foods Ingredients (Videbæk, Denmark). Calcium chloride dihydrate ($CaCl_2 \cdot 2H_2O$; Synth, cat. no. 01C2013.01), calcium hydrogen phosphate ($CaHPO_4$; Sigma-Aldrich, CAS 7757-93-9), trisodium citrate dihydrate ($Na_3C_6H_5O_7 \cdot 2H_2O$; Sigma-Aldrich, CAS 6132-04-3), and 3-(4,5-dimethylthiazol-2-yl)-2,5-diphenyltetrazolium bromide (MTT; Sigma-Aldrich, CAS 57360-69-7) were used in the cytotoxicity and transport experiments. Hanks' balanced salt solution (HBSS) used as the receiving solution was calcium-free. Unless stated otherwise, cell culture reagents and buffers were prepared using the suppliers' instructions.

### 2.2 IoC design, fabrication, flow testing and sterilization

The intestine-on-chip (IoC) designs were developed in AutoCAD® with reference to previously described microfluidic and intestine-on-chip systems [16, 24]. Two designs were fabricated: a single-use acrylic IoC (SuA) and a reusable polydimethylsiloxane IoC (RPDMS). The devices consisted of apical and basal channels separated by a polyester cell-culture membrane (IP Cell Culture™, 0.2-µm pore size). Pipette tips were used to form the inlets and outlets, and ARcare® adhesive tape and PVC adhesive were used during assembly. The SuA device was assembled from laser-cut acrylic components. The RPDMS device incorporated molded PDMS channel layers, acrylic components, adhesive tape, and four bolt-and-nut sets for sealing and disassembly. Device designs, dimensions, and assembly are shown in **Fig. 1**.

A Kawai 13 Combat laser cutter was used to cut device components. The recorded settings were 90% power, 40% speed, and 85% corner power. PDMS components for the RPDMS device were prepared by replica molding. Device components were manually assembled.

Devices were tested for leakage and channel crossflow using syringe pumps (NE-300 and NE-1000; New Era Pump Systems) and water-soluble food dyes introduced separately into the apical and basal channels. Devices showing leakage, crossflow, or structural failure were excluded. For cell culture, medium was perfused at 1 µL/min. For nutrient-transport experiments, the apical test solution and basal HBSS were perfused at 10 µL/min.

After cutting, device components were washed with detergent and running water and exposed to UV-C irradiation for 3 h. Following assembly, channels were flushed with ethanol and then culture medium before cell seeding. Acrylic components were not autoclaved because they deformed under the conditions tested.

### 2.3 Caco-2 cell culture and cytotoxicity assay

Caco-2 cells (ATCC® HTB-37™), originally obtained from Dra. Rosângela M. N. Bezerra (UNICAMP, Limeira, Brazil), were maintained in Corning® culture flasks (cat. no. 430372). Cells were routinely passaged weekly using 0.25% trypsin-EDTA (Sigma-Aldrich, cat. no. T4549). The culture medium was high-glucose DMEM (4,500 mg/L glucose) containing L-glutamine and no pyruvate (Gibco/Invitrogen, cat. no. 41965-039), supplemented with 10% fetal bovine serum (Vitrocell Embriolife), 1% non-essential amino acids from a 100× stock solution (Gibco/Invitrogen, cat. no. 11140-035), and 1% penicillin-streptomycin from a 100x stock solution (10,000 U/mL penicillin and 10,000 µg/mL streptomycin; Gibco/Invitrogen, cat. no. 15140-122). Cells used in experiments were at passages 50-70.

Cytotoxicity was assessed by an MTT assay. Caco-2 cells were seeded in 96-well tissue-culture-treated plates (Corning®, cat. no. 3997) at $3 \times 10^5$ cells/mL and incubated at 37 °C under 5% CO2. After 24 h, the culture medium was replaced with test solutions prepared in HBSS: $CaCl_2$ at concentrations from 0 to 0.05 mol/L; 60% phenol solution as a positive control; $CaHPO_4$ (0.002 g/mL); trisodium citrate (0.0094 g/mL); Peptigen® (0.01 g/mL); or Peptigen® with $CaCl_2 \cdot 2H_2O$ (0.03 mol/L); the supersaturated calcium formulations followed published preparations [25]. Cells were exposed to the test solutions for 2 h at 37 °C, washed with phosphate-buffered saline (PBS), and incubated with MTT solution (1 mg/mL) for 3 h. After removal of MTT, ethanol/isopropanol/PBS (25:37.5:37.5, v/v/v) was added, and absorbance was measured at 570 nm using a Multiskan GO spectrophotometer (Thermo Scientific).

The survival index (SI) was calculated relative to the negative-control absorbance:

$$SI\ (\%) = {}^{Asample\ .\ 100}/_{Anegative\ control}$$

Where SI is the percent of survival, $A_{sample}$ is the absorbance's average (of each sample) and $A_{negative\ control}$ is the absorbance of the negative control. The assay followed the supplier's protocol [26].

### 2.4 Cell characterization and viability

Cells were counted before seeding using trypan-blue exclusion [27]. For chip culture, Caco-2 cells were suspended at $3 \times 10^6$ cells/mL and introduced into the devices. After a 5-h attachment period at 37 °C and 5% $CO_2$, culture medium was perfused at 1 µL/min. Cell growth was monitored by optical microscopy. Transwell® cultures were maintained under static conditions; monolayer formation was assessed over the culture period.

Cell viability on the Transwell® and IoC supports was assessed using a LIVE/DEAD™ Viability/Cytotoxicity Kit (Invitrogen™, cat. no. L3224) [28]. Calcein AM (1:1,000) and ethidium homodimer-1 (1:2,000) were prepared in PBS, applied to the cells for 30 min, and followed by three PBS washes. Fluorescence images were acquired using a Zeiss LSM 780 confocal microscope. At least three fields per treatment were imaged, each covering 400 × 400 µm and acquired at 1,024 × 1,024 pixels. Image segmentation was performed using ImageJ.

Barrier integrity was assessed by phenol-red diffusion and immunofluorescence for zonula occludens-1 (ZO-1), with DAPI nuclear counterstaining [29]. For the diffusion assay, phenol red (10 µmol/L in HBSS) was added to the apical compartment and HBSS to the basal compartment. Transwell® plates were incubated at 37 °C for 60 min with gentle agitation. Basal samples were transferred to a 96-well plate and absorbance was measured at 558 nm using a Multiskan GO spectrophotometer. Phenol-red concentrations were determined from a calibration curve. Percentage diffusion was calculated as:

$$\text{Diffusion}(\%) = \frac{C_{\mathrm{b},60} - C_{\mathrm{b},0}}{C_{\mathrm{a},0}} \times 100$$

where $C_{b,0}$ and $C_{b,60}$ are the basal phenol-red concentrations at 0 and 60 min, respectively, and $C_{a,0}$ is the initial apical concentration. Apparent permeability (Papp) was calculated as:

$$P_{app} = \frac{V_r}{A\, C_{d,0}} \frac{dC_r}{dt}$$

where $V_r$ is receiver-compartment volume, $A$ is membrane area, $C_{d,0}$ is initial donor-compartment concentration, and $dC_r/dt$ is the rate of change in receiver-compartment concentration.

ZO-1 immunofluorescence was performed using a ZO-1 monoclonal antibody conjugated to Alexa Fluor 488 (Invitrogen, cat. no. 339188) and DAPI (Thermo Fisher, cat. no. 62248).

### 2.5 Nutrient transport experiments

Transport experiments were performed using Caco-2 monolayers in Transwell® inserts and in the SuA and RPDMS devices. Before testing, monolayers were washed three times with HBSS. The test solutions were Peptigen® alone (Pep), Peptigen® with CaCl2 (PepCa), and CaCl2 alone (Ca). In Transwell® experiments, solutions were tested in triplicate wells. Initial apical and basal samples were collected, and the plates were incubated at 37 °C for 60 min with mild agitation before final samples were collected.

For chip experiments, three SuA and three RPDMS devices were evaluated per test solution. Following confirmation of monolayer integrity and an HBSS wash, the test solution was perfused through the apical channel and calcium-free HBSS through the basal channel at 10

184 μL/min. Outlet samples were collected over 60 min at 37 °C. The three test solutions were run
185 sequentially, with HBSS washing between solutions.
186
187 **2.6 Calcium quantification by direct-injection ESI-MS**
188 Calcium was quantified by direct-injection electrospray ionization mass spectrometry
189 (DI-ESI-MS) following complexation with EDTA [30]. Each sample (50 μL, diluted in HBSS as
190 required) was mixed with 50 μL of 30 mmol/L EDTA in aqueous $NH_3/NH_4Cl$ buffer (pH 10).
191 Calcium standards were prepared and analyzed using the same procedure.
192 Analyses were performed using a Thermo Scientific LTQ Orbitrap Velos mass
193 spectrometer fitted with a heated electrospray ionization (HESI) source. Samples were
194 introduced directly at 30 μL/min using water containing 10% methanol as the mobile phase. Data
195 were acquired in negative-ion mode over m/z 150-1,000, with selected-ion monitoring of m/z
196 291 and 329. The reported source voltage was 2.5 kV; capillary and heater temperatures were
197 200 °C and 150 °C, respectively.
198 Calcium concentrations were determined from the extracted-ion chromatogram peak area
199 for m/z 329, corresponding to the calcium-EDTA complex, using an external calibration curve.
200 The free EDTA signal at m/z 291 was also monitored. Calibration standards and samples were
201 analyzed in triplicate. The linear range, limit of detection (LOD), and limit of quantification
202 (LOQ) were determined for the method. Calcium concentrations were corrected for dilution
203 before calculation of Papp.
204
205
206

### 2.7 Peptide analysis by MALDI-TOF/TOF-MS/MS

Peptide-containing samples were analyzed using an Autoflex Max MALDI-TOF/TOF mass spectrometer (Bruker Daltonics, Bremen, Germany). The matrix was α-cyano-4-hydroxycinnamic acid in 50% acetonitrile/50% water containing 0.1% trifluoroacetic acid. Angiotensin I (Sigma-Aldrich, cat. no. 70937-97-2) was added as an internal reference at a final concentration of 0.5 μmol/L; peptide signal intensities were normalized to the angiotensin I signal at m/z 1,296.

Monoisotopic peptide masses were acquired in positive reflector mode over m/z 500-3,500, and tandem mass spectra were obtained in LIFT mode. MALDI-TOF data were externally calibrated. Peptide assignments were evaluated using a non-specific-digestion search in MaxQuant, with a precursor tolerance of 0.2 Da and fragment tolerance of 0.50 Da. Sequence assignments were compared with bovine protein entries in Swiss-Prot, UniProt, Protein BLAST, and Protein Prospector. The assignments were also compared with a previously generated nLC-MS/MS peptidome dataset for Peptigen® (**Supplementary Table 2).**

Ions detected in at least two of three samples and absent from the HBSS blank were retained for evaluation. Apical and basal signals were compared to identify peptides present in transport samples. Peptide Papp was calculated using the apical concentration as the donor concentration. Candidate calcium adducts were screened by comparing observed mass differences with the expected mass shifts for one or two calcium ions.

### 2.8 Confirmation of candidate calcium-adduct assignments

Candidate ions approximately 38 Da above the protonated peptide mass were assessed as possible calcium adducts, $[M - H + Ca]^+$, or potassium adducts, $[M + K]^+$. Because the

calculated mass difference between these assignments was below the mass accuracy available from external calibration on the axial time-of-flight instrument, mass measurement alone was not used to distinguish them. Candidate isotopic envelopes were compared with theoretical distributions calculated for the calcium- and potassium-containing compositions. In addition, basolateral samples were spiked separately with $CaCl_2$ and KCl, and the effects on candidate-ion signals were assessed.

### 2.9 Human and animal rights

Human and animal rights. This study did not involve human participants or animals. All experiments were performed in vitro using the established Caco-2 cell line (ATCC HTB-37), derived from a human colorectal adenocarcinoma and obtained as described above; no primary human material was collected for this work, and no informed consent was therefore required.

### 2.10 Use of generative AI

Generative AI (ChatGPT, OpenAI) was used to assist with restructuring and language editing of the manuscript, and check for internal numerical consistence. The authors revised the text and take full responsibility for its content.

## 3 Results

### 3.1 IoC fabrication and flow performance

Two intestine-on-a-chip devices were fabricated: the single-use acrylic IoC (SuA) and the reusable PDMS IoC (RPDMS). Both devices had apical and basal channels separated by a porous polyester membrane, with pipette-tip inlets and outlets. The SuA device was assembled

from acrylic components, whereas the RPDMS device incorporated molded PDMS channel layers, acrylic covers, adhesive tape, and four bolt-and-nut sets. Device designs, dimensions, representative photographs, and the fabrication and cleaning workflow are shown in **Fig. 1**.

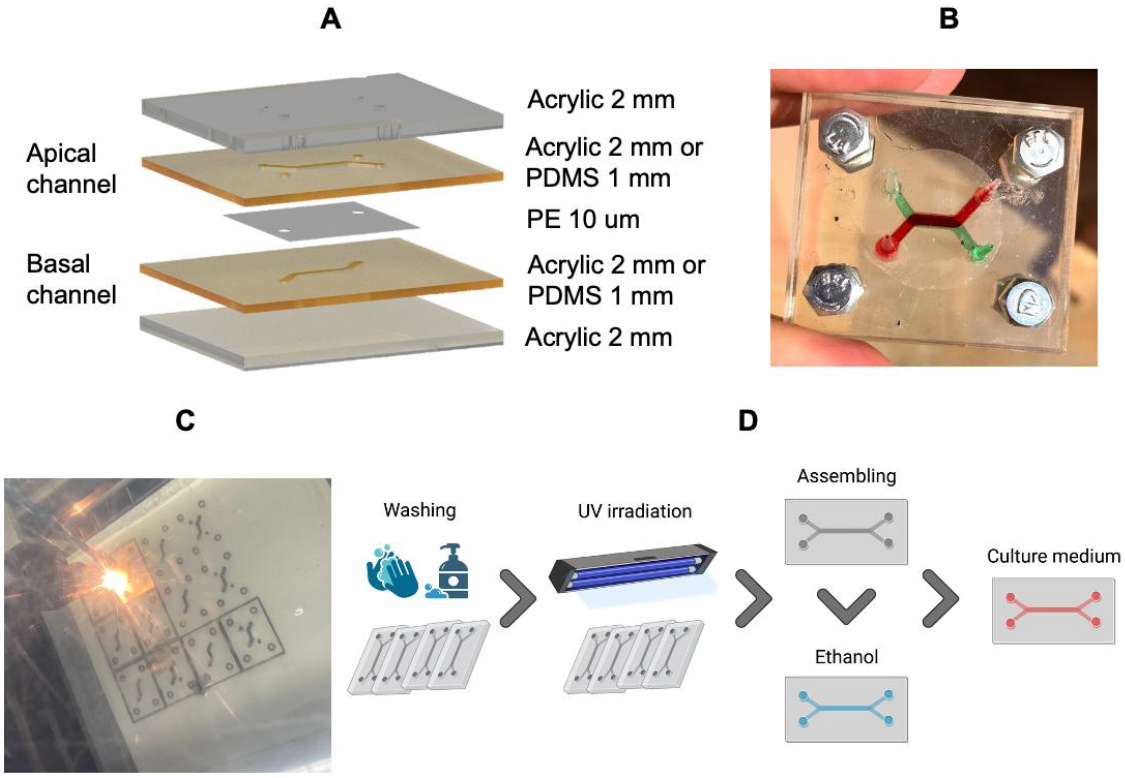



***Figure 1.*** *Design, fabrication, and sterilization of the intestine-on-a-chip devices. (A) Device schematics and dimensions. (B) Photograph of the RPDMS device after dye-flow testing. (C) Laser-cutting process for SuA device components. (D) Device cleaning and sterilization workflow.*

Both designs passed visual dye-flow tests for leakage and crossflow and supported flow rates up to 50 µL/min without collapsing. Some devices became contaminated during testing, particularly around device openings. The estimated material cost per device was US$0.80 for SuA and US$3.74 for RPDMS. These estimates exclude labor and laser-cutter energy costs; the

RPDMS device was designed for disassembly and reuse. Material costs are summarized in Table 1.

***Table 1.*** *Estimated material costs per SuA and RPDMS device.*

| Material | General Cost (US$) | Cost per Unit SuA (US$) | Cost per Unit RPDMS (US$) |
|---|---|---|---|
| **Acrylic board (0.002/1/2 m)** | 80 | 0.22 | 0.16 |
| **PDMS (0.5kg)** | 125 | ----- | 0.60 |
| **Arcare tape[1]** | ----- | ----- | ----- |
| **Pipette tips (1000 pack)** | 90 | 0.36 | 0.36 |
| **Nut and bolt (50 pack)** | 15 | ---- | 2.40 |
| **Membrane[2] (10-sheet pack)** | 430 | 0.22 | 0.22 |
| **Final cost (per chip)** | ----- | 0.80 | 3.74 |

1 Arcare tape was donated by Adhesives Research® (Glen Rock, PA, US); however, it was not available for costumer sale.

2 Membrane prices will vary according to the specifications. For this estimation, a PE track-etched transparent membrane sheet from IP Cell CultureTM was used for calculations.

During cell culture, medium was perfused at 1 µL/min. Nutrient-transport experiments were conducted at 10 µL/min to obtain sufficient outlet sample for analysis. After eight days of perfused culture, microscopy showed attached cells forming a continuous or nearly continuous layer in both IoC designs. The flow rates and corresponding calculated shear stress are provided in **Online Resource 1**.

### 3.2 Cytotoxicity of the test solutions

The MTT assay was used to assess Caco-2 responses to the solutions considered for the transport experiments. Peptigen® alone, $CaCl_2$ solutions, and the Peptigen®-$CaCl_2$ combination did not reduce the survival index relative to the negative control under the tested exposure conditions (**Fig. 2A-C**). The supersaturated formulations containing calcium phosphate and

285 citrate reduced the survival index; citrate alone did not show the same reduction. On this basis,
286 calcium enrichment with $CaCl_2$ was used for the subsequent transport experiments.
287
288 **3.3 Caco-2 growth, viability, and barrier assessment**
289 Caco-2 monolayer formation was assessed on Transwell® inserts and in both IoC
290 designs. By day 8, cells in the perfused devices covered most of the membrane surface.
291 Transwell® cultures showed more extensive uncovered areas at day 8; near-complete coverage
292 was observed by day 21 (**Fig. 2D**).
293 Live/dead staining showed that most of the imaged area was occupied by viable cells on
294 all three supports. Image-based segmentation estimated viable-cell coverage above 90% (**Online**
295 **Resource 2**). The approximate cell-layer thickness was 15-20 μm on Transwell® inserts and 20-
296 25 μm in the IoC devices; estimates for the chips were less certain because of light scattering
297 from the device materials (**Fig. 2E**).
298 Phenol-red diffusion was below 5% for the tested monolayers, and calculated Papp
299 values were below $10^{-5}$ cm/s (Fig. 2F). ZO-1 staining with DAPI counterstaining showed
300 junctional staining and cell coverage on Transwell®, SuA, and RPDMS supports (**Fig. 3**). Image
301 resolution on the chips was reduced by light scattering from the device materials.

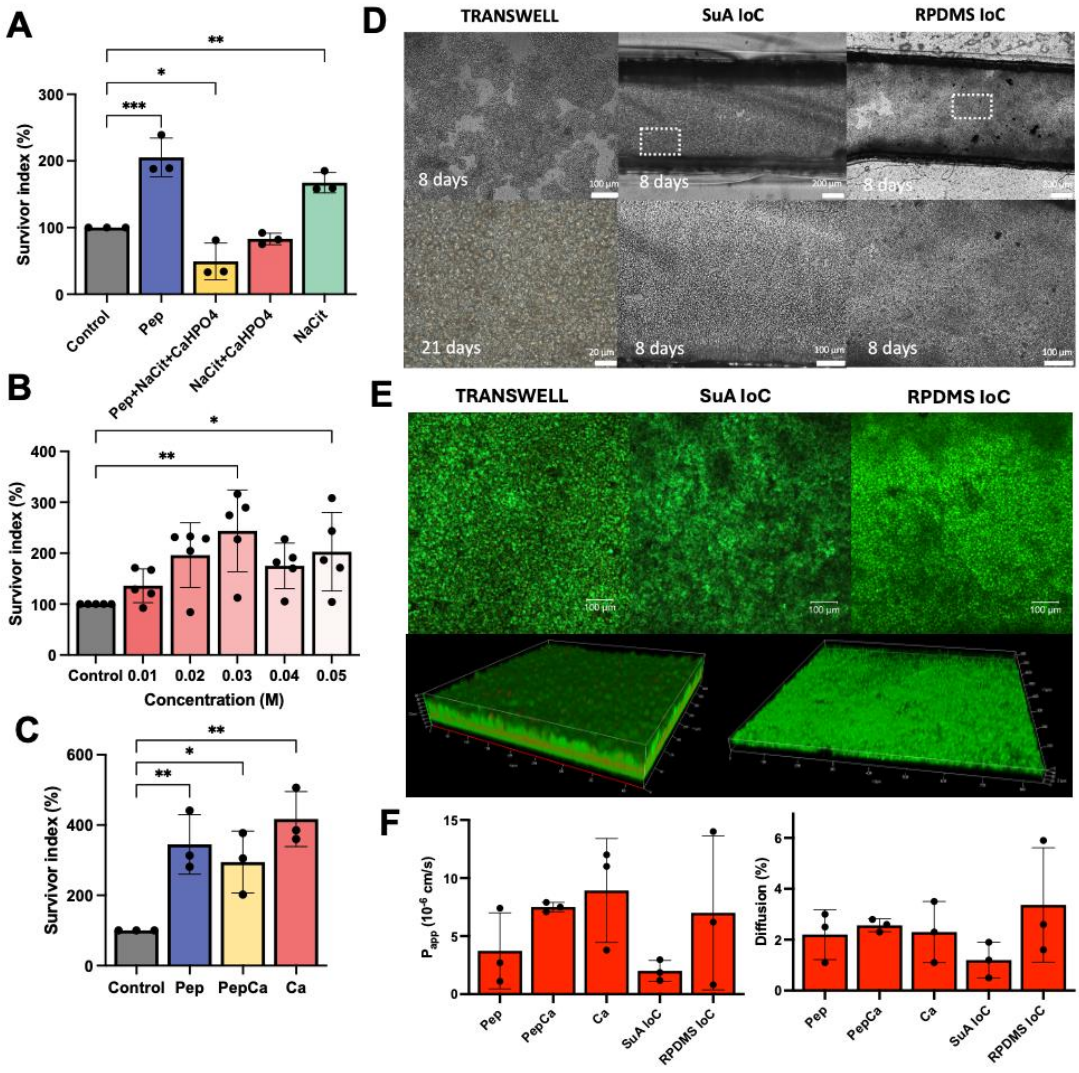



***Figure. 2.*** *Characterization of Caco-2 cells across the three culture platforms. (A-C) Survival index for test solutions. (D) Representative micrographs of cell growth under static Transwell® and perfused SuA and RPDMS conditions. (E) Live/dead confocal images and representative three-dimensional reconstructions. (F) Phenol-red apparent permeability and percentage diffusion.*

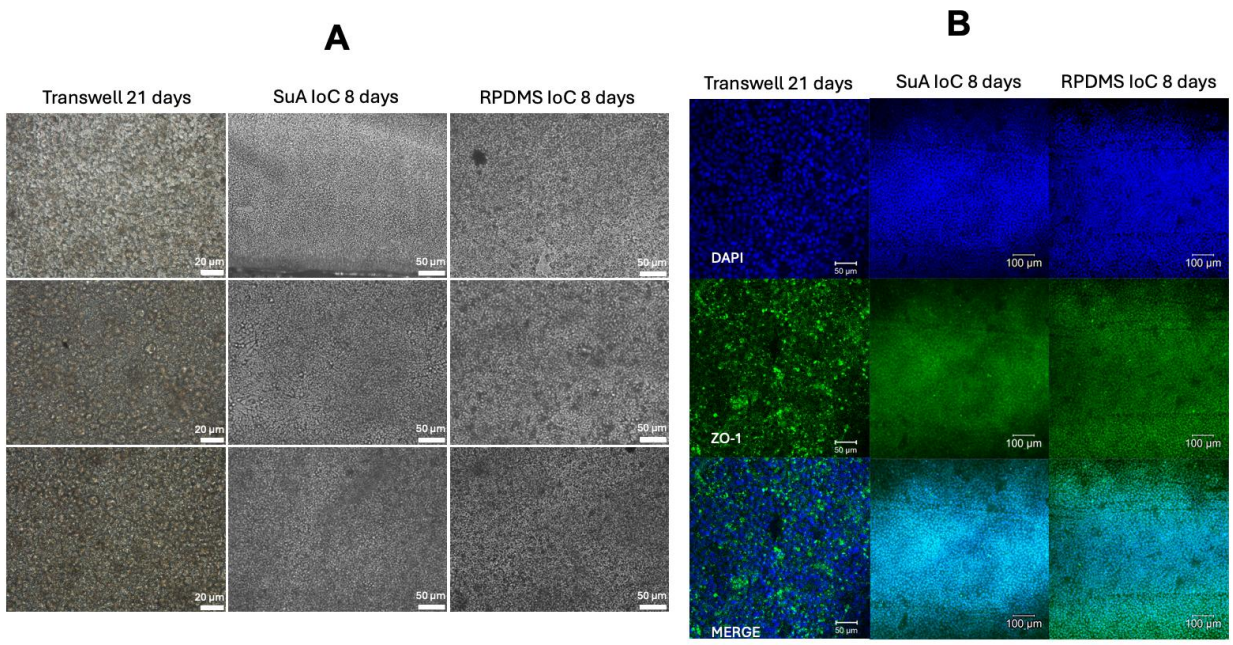



***Figure 3****. Caco-2 monolayers on Transwell®, SuA, and RPDMS supports. (A) Bright-field images of replicate monolayers. (B) Confocal images following ZO-1 immunostaining and DAPI counterstaining.*

### 3.4 Calcium transport

Calcium was quantified as its EDTA complex, monitored at *m/z* 329. The calibration response was linear over the 0-5 mM working range. The LOD and LOQ were 0.21 ± 0.06 mM and 0.63 ± 0.17 mM, respectively (**Fig. 4A-D**).

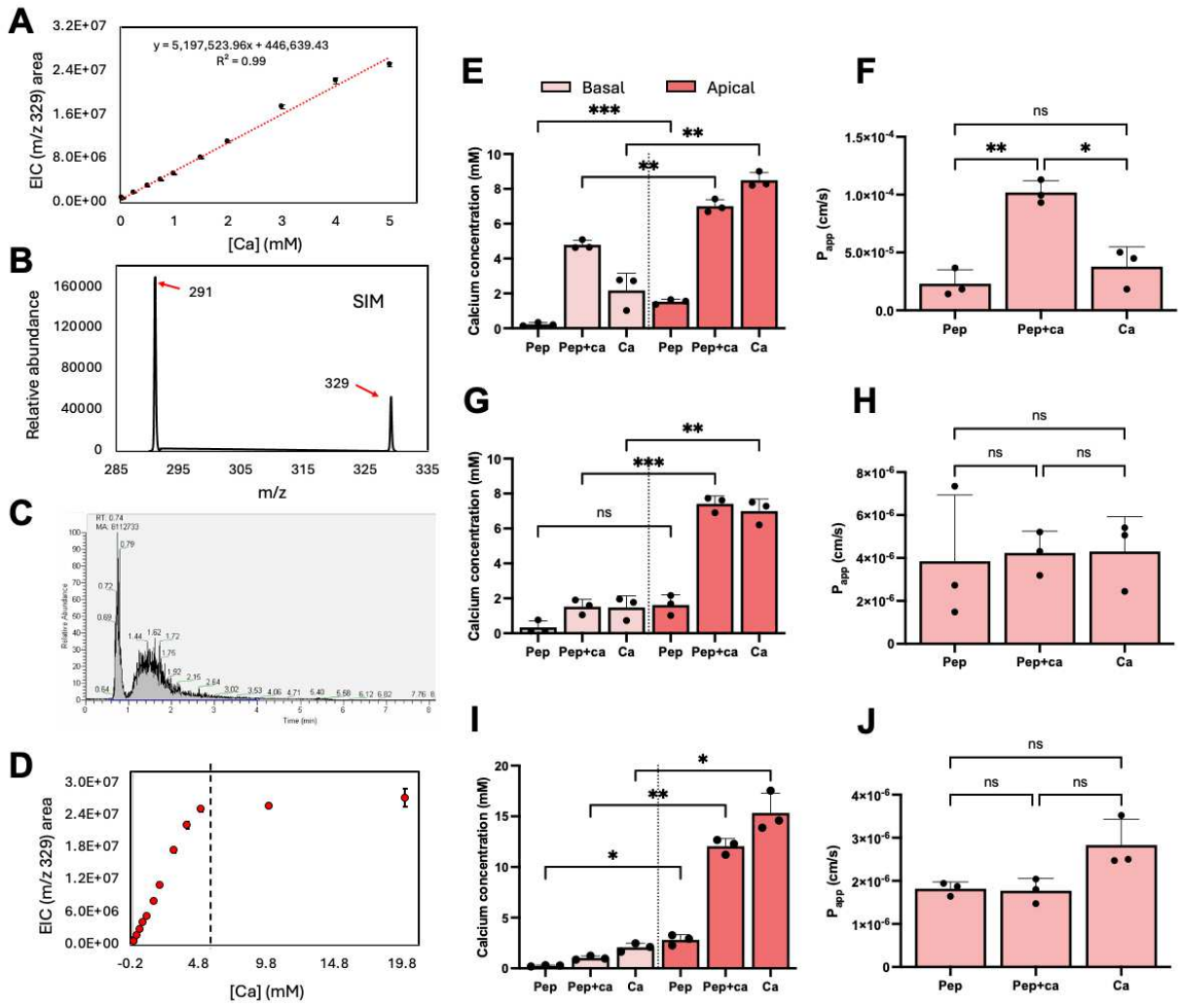
In Transwell® experiments, the basolateral calcium concentration was 4.8 ± 0.3 mM for Peptigen® plus $CaCl_2$ (PepCa), 2.2 ± 0.1 mM for $CaCl_2$ alone (Ca), and 0.2 ± 0.09 mM for Peptigen® alone (Pep) (Fig. 4E). The Pep value was at or below the method's LOD and is therefore reported as an estimate rather than a quantified concentration. Corresponding Papp values were 10.2 ± 1.0 × $10^{-5}$ cm/s for PepCa, 3.8 ± 1.7 × $10^{-5}$ cm/s for Ca, and 2.3 ± 1.2 × $10^{-5}$

cm/s for Pep (**Fig. 4F**). PepCa had a significantly higher Papp than both Ca and Pep, as reported in the original analysis. PepCa and Ca contained the same nominal calcium load.

In SuA experiments, basolateral calcium concentrations were 1.5 ± 0.4 mM for PepCa, 1.5 ± 0.6 mM for Ca, and 0.3 ± 0.3 mM for Pep (**Fig. 4G**). Differences in calcium transport among the three solutions were not statistically significant. The relatively high variability for Pep reflected variation among devices.

In RPDMS experiments, basolateral calcium concentrations were 1.0 ± 0.2 mM for PepCa, 2.1 ± 0.4 mM for Ca, and 0.2 ± 0.06 mM for Pep (Fig. 4I). The Pep value was at or below the LOD. The corresponding Papp values were $1.8 \pm 0.3 \times 10^{-6}$ cm/s for PepCa, $2.8 \pm 0.6 \times 10^{-6}$ cm/s for Ca, and $1.8 \pm 0.2 \times 10^{-6}$ cm/s for Pep (**Fig. 4J**). Treatment differences were not statistically significant. Thus, the ranking of PepCa and Ca in RPDMS differed from that observed in the Transwell® system.

Comparisons among platforms showed significant differences in Papp, as reported in the original analysis (Brown-Forsythe and Welch's ANOVA, $p < 0.0001$). Across all three platforms, the recovered calcium concentration was higher for PepCa than for Pep. However, the treatment ranking and statistical significance of the PepCa-versus-Ca comparison were not consistent across platforms.




339

340 ***Figure 4.*** *Calcium analysis and transport results. (A) Calcium-EDTA calibration curve. (B)*
341 *Representative mass spectrum of a calcium-EDTA sample. (C) Representative extracted-ion*
342 *chromatogram used for quantification. (D) Calibration response across the tested concentration*
343 *range. (E-F) Transwell® calcium concentrations and Papp values. (G-H) SuA calcium*
344 *concentrations and Papp values. (I-J) RPDMS calcium concentrations and Papp values. P*
345 *values: * < 0.05, ** < 0.005, *** < 0.0005.*

346

347

348

### 3.5 Peptide profiles and candidate calcium adducts

MALDI-TOF/TOF-MS/MS analysis detected peptides in samples from the Transwell®, SuA, and RPDMS experiments. The full peptide assignments and calculated Papp values for each platform are provided in Online Resources 3-5. Representative spectra are shown in Online Resource 6.

Among the peptide ions examined, two casein-derived sequences were consistently assigned with high confidence: β-casein f59-68, VYPFPGPIPN, and κ-casein f107-121, AIPPKKNQDKTEIPT. Ions with mass shifts consistent with calcium adducts were detected in apical and/or basal samples. The complete mass comparisons, sequence assignments, and sample locations are presented in the corresponding Online Resource tables. The structures and proposed candidate binding sites for the two peptides are shown in **Fig. 5**.

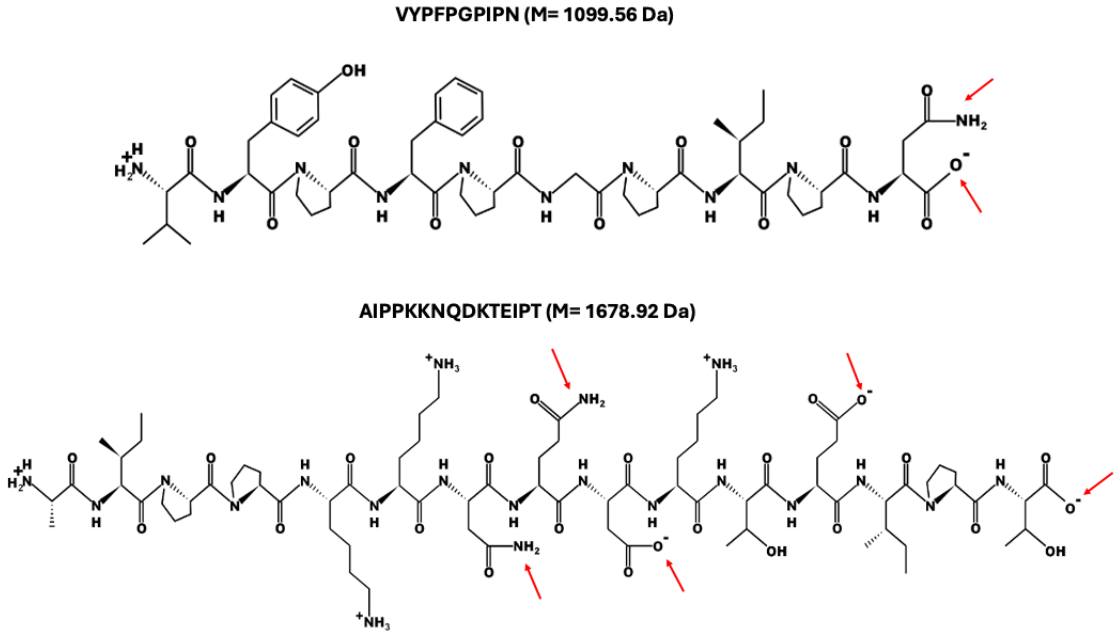



***Figure 5.*** *Structures of the casein-derived peptides VYPFPGPIPN and AIPPKKNQDKTEIPT, showing proposed potential calcium-coordination sites.*

The candidate ions were evaluated as potential calcium rather than potassium adducts using their isotopic envelopes and separate $CaCl_2$ and KCl spike tests. The observed isotopic envelopes matched the calculated calcium-adduct distributions. Spiking basolateral samples with $CaCl_2$ increased the signal of the candidate 38-Da species, whereas KCl spiking did not. These results support assigning the detected adduct species as calcium adducts. They do not, by themselves, establish whether the peptide-calcium complexes crossed the cell monolayer intact or formed after transport during sample handling or ionization.

# 4 Discussion

## 4.1 Calcium transport in the presence of whey protein hydrolysate

The clearest treatment difference was observed in the Transwell® system. At the same nominal apical calcium concentration (30 mM), the apparent permeability of calcium in the presence of Peptigen® was approximately 2.7-fold that measured for CaCl2 alone. This result is consistent with the effect of the hydrolysate matrix on calcium transport under the conditions tested. However, the experiment does not identify the mechanism responsible for that difference. The hydrolysate may affect calcium solubility or speciation, interact with the epithelial barrier, or influence transport through other matrix-dependent effects.

The receiving compartment contained calcium-free HBSS, reducing calcium background in the receiver samples. The comparison between PepCa and Ca was made under the same nominal calcium conditions, so the higher Transwell® Papp for PepCa cannot be explained by a difference in the added apical calcium concentration. The assay measured calcium recovered in the receiver after EDTA complexation; it did not distinguish free calcium from calcium associated with other components before analysis.

One possible explanation is that peptides in the hydrolysate help maintain calcium in a soluble form. In the intestinal lumen, calcium solubility can be affected by interactions with phosphate, carbonate, and other dietary components [8, 10]. Peptide ligands containing suitable coordinating groups may alter calcium speciation and reduce precipitation under some conditions [25, 31]. In this study, the $CaHPO_4$/citrate formulations reduced the Caco-2 survival index under the conditions tested, whereas the Peptigen®-CaCl2 solution did not. This supports using the latter formulation in the transport experiments, but the cytotoxicity assay does not itself demonstrate improved calcium solubility or bioavailability.

A second possibility is that calcium associated with peptides contributes to transport. Peptide ions assigned as calcium adducts were detected in transport samples, but the mass-spectrometric results alone cannot establish whether the complexes crossed the monolayer intact. This distinction is discussed in Sect. 4.4. The principal transport result, the higher apparent calcium permeability for PepCa than for Ca in Transwell®, does not depend on proving intact complex transport.

Milk-derived calcium-binding peptides have often been studied in the context of casein phosphopeptides, whose phosphorylated residues can coordinate calcium [32, 33]. The two casein-derived sequences examined here were assigned as non-phosphorylated peptides. Their detection therefore raises the possibility that calcium association may also occur with non-phosphorylated milk-protein fragments, although their contribution to calcium transport requires further investigation.

### 4.2 Perfusion and Caco-2 monolayer formation

Caco-2 monolayers in the perfused devices showed extensive surface coverage by day 8, whereas near-complete coverage in the Transwell® system was observed by day 21. The chip monolayers also showed ZO-1 staining and low phenol-red diffusion, consistent with formation of a barrier under the assessment conditions. These results suggest that the perfused culture conditions supported earlier formation of a confluent, barrier-competent layer in this study.

The evidence does not establish full enterocyte differentiation or functional maturation of calcium-transport pathways. Brush-border enzyme activity and expression of calcium-transport proteins such as TRPV6, calbindin-D9k, and PMCA1b were not measured. Therefore, the observed difference concerns cell coverage and barrier-related measures; whether perfusion also accelerated functional maturation remains unknown. This distinction is important because barrier formation and nutrient-transport capacity are not necessarily equivalent [14].

### 4.3 Casein-derived peptides detected in transport samples

Two casein-derived sequences were assigned with high confidence in the peptide analysis: κ-casein f107-121 (AIPPKKNQDKTEIPT) and β-casein f59-68 (VYPFPGPIPN; corresponding to f74-83 when numbered using the precursor sequence). Their mass shifts were consistent with calcium-adduct assignments under the analytical conditions used.

The κ-casein sequence is located at the N-terminal region of caseinomacropeptide (CMP), which is released during rennet coagulation and is present in sweet whey [34]. Its detection is therefore compatible with the dairy origin of the whey ingredient. The detected sequence lacks the N-terminal methionine of the longer CMP segment. Its observed mass was consistent with the unglycosylated form, and the phosphorylation sites described for κ-casein

occur outside this sequence [35, 36]. These features are relevant to interpreting its potential calcium association, but the present experiments do not establish the peptide's binding affinity or its functional contribution to calcium transport.

The second sequence, VYPFPGPIPN, is a β-casein-derived peptide in the β-casomorphin region [37]. It contains no aspartate, glutamate, or phosphoserine residues. Calcium coordination is therefore less readily attributed to the side-chain carboxylate groups commonly implicated in peptide-calcium binding. Backbone carbonyls and other available groups may contribute to metal-ion association, but the proposed interaction should be considered provisional [31, 38]. On this basis, the κ-casein fragment is the more plausible candidate calcium-binding peptide, while the assignment of VYPFPGPIPN as a carrier warrants caution.

### 4.4 Calcium-adduct assignments and their interpretation

Candidate ions approximately 38 Da above the protonated peptide masses were evaluated as possible as calcium adducts, $[M - H + Ca]^+$, rather than potassium adducts, $[M + K]^+$. Because the mass difference between these alternatives was below the accuracy available from external calibration on the axial time-of-flight instrument, mass measurement alone was insufficient for assignment.

The isotopic envelopes of the candidate ions were consistent with the calculated calcium-containing compositions. In addition, $CaCl_2$ spiking increased the signal of the candidate 38-Da species, whereas KCl spiking did not. Taken together, these tests support assigning the detected species as calcium adducts.

This assignment identifies the adducted element, but it does not establish when the adduct formed. The increase in adduct signal following calcium spiking also demonstrates that peptide-

calcium adducts can form during sample handling or analysis. Thus, a calcium-adduct signal in a basal sample could represent a complex that crossed the monolayer, or a peptide that crossed and subsequently associated with calcium before or during mass-spectrometric analysis. The available data does not distinguish these possibilities.

A useful follow-up would be to characterize the relationship between free calcium concentration and the adduct-to-precursor signal ratio in basolateral samples. Comparing that calibration with unspiked transport samples could help assess whether the observed adduct abundance exceeds what would be expected from post-transport adduct formation. This approach would still require careful validation under the same sample preparation and instrumental conditions.

### 4.5 Possible routes of calcium transport

In Transwell® experiments, the apparent permeability calculated for calcium was higher than that measured for phenol red. This difference may reflect the distinct properties of the analytes, but it does not by itself establish the route of calcium transport. Phenol red and calcium differ in size, charge, binding, and transport behavior; permeability comparisons between them should therefore be interpreted cautiously.

A transcellular contribution is possible. Caco-2 cells can express components associated with transcellular calcium transport, including TRPV6 and calbindin-D9k, although their expression and function may differ from those in native small-intestinal enterocytes [39, 40]. However, these transport proteins were not measured in the present study.

The use of calcium-free HBSS in the receiving compartment is another consideration. Calcium depletion can affect cell-cell adhesion and epithelial barrier properties in some

experimental settings. If the barrier changed during the 60-min transport assay, phenol-red permeability measured separately might not fully represent barrier permeability during calcium transport. This possibility was not tested directly. The PepCa-versus-Ca comparison was conducted with the same nominal apical calcium load and the same calcium-free receiving solution, so the buffer condition was shared by those two treatments; nonetheless, its effects on barrier function cannot be ruled out.

Experiments using temperature variation, bidirectional transport, calcium-transport inhibitors or knockdown, and measurement of relevant transporter expression would help clarify the route. Such studies would also benefit from monitoring barrier integrity throughout the transport experiment rather than only before or after it.

### 4.6 Physiological relevance and study limitations

Several features of the experimental model limit direct translation to human calcium absorption.

First, the nominal apical calcium concentration was 30 mM, and the receiving solution was calcium-free HBSS. These conditions were used for analytical measurement and to reduce receiver-side background, but they create a concentration gradient unlike that in vivo. The persistence and magnitude of the observed PepCa-versus-Ca difference at lower, more physiologically relevant calcium concentrations remain to be established.

Second, the whey protein hydrolysate was applied directly to the Caco-2 monolayers without prior simulated gastrointestinal digestion. Although Peptigen® is already hydrolyzed, in vivo it would undergo further exposure to gastric, pancreatic, and brush-border digestion.

Testing the ingredient after standardized simulated digestion, such as an INFOGEST protocol [41], would be an important next step [42].

Third, Caco-2 cells are derived from a colorectal adenocarcinoma and do not reproduce all features of the small-intestinal epithelium. The cultures also lacked a mucus-producing co-culture component. Future studies could evaluate additional intestinal models, including mucus-producing co-cultures or small-intestinal cell models, and characterize the expression of calcium-transport machinery [43].

Accordingly, the present findings show a difference in measured calcium transport in one in vitro configuration; they do not establish increased human calcium bioavailability. Whether the effect persists after digestion and at physiologically relevant calcium concentrations requires further study.

### 4.7 Platform performance and implications

The two IoC designs supported perfused Caco-2 culture and enabled collection of samples for calcium and peptide analysis. However, their calcium-transport results did not reproduce the Transwell® treatment ranking consistently. In SuA, PepCa and Ca produced similar mean basolateral calcium concentrations, with no statistically significant treatment differences. In RPDMS, the mean concentration for Ca was higher than for PepCa, also without a significant treatment difference. Thus, the chip results demonstrate the feasibility of the platform for this type of experiment but do not independently confirm the Transwell® PepCa-versus-Ca result.

Manual fabrication, variation in channel dimensions, membrane placement, and sealing may contribute to a between-device variability. The small number of devices per treatment also

limits statistical power. Although PDMS-related analyte sorption is a possible consideration, it was not directly measured in this study and should be treated as a hypothesis rather than an established explanation for the RPDMS results.

The estimated device costs were US$0.80 for SuA and US$3.74 for RPDMS, based on materials and excluding labor and laser-cutter energy. These estimates indicate low material costs but should not be interpreted as full operating costs. The RPDMS design is reusable, though its practical lifetime and performance across repeated sterilization and use cycles were not quantified.

Overall, the IoC devices provided a low-cost, perfused format for Caco-2 culture and nutrient-transport sampling. Improving fabrication consistency, increasing replication, and evaluating device performance across repeated use will be necessary before the platforms can support robust comparisons among food ingredients.

## 5 Conclusions

At the same nominal apical calcium load, the apparent calcium permeability measured in the Transwell® system was higher when calcium was supplied with Peptigen® than when supplied as $CaCl_2$ alone. This result supports an effect of the hydrolysate matrix on calcium transport under the conditions tested but does not establish the mechanism or predict human bioavailability. The corresponding treatment differences in the two IoC devices were not statistically significant, and the PepCa-versus-Ca ranking was not consistent across platforms.

Two casein-derived peptide sequences, κ-casein f107-121 and β-casein f59-68, were detected and assigned as candidate calcium-adduct species. The results support their association

with calcium under the analytical conditions used but do not demonstrate that intact peptide-calcium complexes crossed the monolayer.

Perfused culture produced Caco-2 layers with extensive coverage and barrier-associated features by day 8, compared with near-complete coverage by day 21 in Transwell® culture. The low-cost devices show potential for perfused food-transport studies, but further work is needed to improve reproducibility and test transport after simulated digestion and at more physiologically relevant calcium concentrations.

## Supplementary Information

The online version contains supplementary material available as Online Resources 1-6, which include:

**Online Resource 1:** Figure S1 showing calculated shear stress for devices #4 and #5 across the tested flow rates, together with representative Caco-2 culture images after 8 days.

**Online Resource 2:** Table S1 showing image-based color-segmentation estimates of live and dead cell areas on the Transwell®, SuA, and RPDMS supports.

**Online Resource 3:** Tables S2-S4 showing peptide assignments, apparent permeability values, and candidate calcium-adduct mass comparisons for the Transwell® experiments.

**Online Resource 4:** Tables S5-S6 showing peptide assignments, apparent permeability values, and candidate calcium-adduct mass comparisons for the SuA device.

**Online Resource 5:** Tables S7-S8 showing peptide assignments, apparent permeability values, and candidate calcium-adduct mass comparisons for the RPDMS device.

**Online Resource 6:** Figure S2 showing representative MALDI-TOF/TOF-MS spectra from peptide-transport experiments.

## Author contributions

Conceptualization: J.F.F, D.R.C, L.H.S.; methodology: J.F.F., S.T.B.M., V.F.G., A.M.L., M.H.L., L.C.B., G.K.; software: J.F.F., S.T.B.M., V.F.G.; validation: J.F.F., S.T.B.M., A.T.B.M; formal analysis: J.F.F., S.T.B.M., V.F.G.; investigation: J.F.F, D.R.C, E.C.; resources: J.F.F.; data curation: J.F.F., S.T.B.M.; writing original draft preparation: J.F.F.; writing, review and editing: J.F.F, L.C.B., L.H.S. D.R.C, E.C.; visualization: J.F.F, L.C.B., D.R.C, E.C.; supervision: D.R.C.; project administration: J.F.F, D.R.C.; funding acquisition, J.F.F, L.H.S., D.R.C.

## Funding

This research was funded by FAPESP, grant number 18/11657-4 and 17-011890, and CNPq (Research Productivity Grant to DRC and EC).

## Acknowledgements

The authors thank Prof. Dr. Rosângela M. N. Bezerra (UNICAMP) for kindly providing the Caco-2 cells used in this study. We are also grateful to Mr. Gabriel José N. Gomes for his assistance in teaching the fundamentals of AutoCAD to J.F.F. In addition, we acknowledge Prof. Francisco E. G. Guimarães (IFSC/USP) for granting access to the confocal fluorescence instrument. This research was part of the PhD thesis of JFF available at https://www.teses.usp.br/teses/disponiveis/75/75133/tde-13122022-104043/pt-br.php [34].

## Declarations

Competing interests. Peptigen® IF3080 was kindly donated by Arla Foods Ingredients (Videbæk, Denmark). The company had no role in the design of the study, in the collection, analysis or interpretation of the data, in the writing of the manuscript, or in the decision to submit it for publication. The authors declare no other financial or non-financial competing interests.

Ethics approval. Not applicable. The study used only an established, commercially available human cell line and involved no human participants or animals.

Consent to participate / Consent for publication. Not applicable.

Data availability. Data is available on request.

## References

1. Bein A, Shin W, Jalili-Firoozinezhad S, Park MH, Sontheimer-Phelps A, Tovaglieri A, Chalkiadaki A, Kim HJ, Ingber DE (2018) Microfluidic Organ-on-a-Chip Models of Human Intestine. Cell Mol Gastroenterol Hepatol 5:659–668. https://doi.org/10.1016/j.jcmgh.2017.12.010

2. Lin SL, Lin TY, Fuh MR (2013) Recent developments in microfluidic chip-based separation devices coupled to MS for bioanalysis. Bioanalysis 5:2567–2580. https://doi.org/10.4155/bio.13.196

3. Bhatia SN, Ingber DE (2014) Microfluidic organs-on-chips. Nat Biotechnol 32:760–772. https://doi.org/10.1038/nbt.2989

4. Imura Y, Asano Y, Sato K, Yoshimura E (2009) A Microfluidic System to Evaluate Intestinal Absorption. Anal Sci 25:1403–1407. https://doi.org/10.2116/analsci.25.1403

613 5. Pocock K, Delon L, Bala V, Rao S, Priest C, Prestidge C, Thierry B (2017) Intestine-on-A-
614 Chip Microfluidic Model for Efficient in Vitro Screening of Oral Chemotherapeutic Uptake.
615 ACS Biomater Sci Eng 3:951–959. https://doi.org/10.1021/acsbiomaterials.7b00023
616 6. Coudray B (2011) The contribution of dairy products to micronutrient intakes in France. J Am
617 Coll Nutr 30:410S-414S. https://doi.org/10.1080/07315724.2011.10719984
618 7. Institute of Medicine (US) Committee to Review Dietary Reference Intakes for Vitamin D and
619 Calcium (2011) Dietary Reference Intakes for Calcium and Vitamin D. National Academies
620 Press, Washington, DC. https://doi.org/10.17226/13050
621 8. Guéguen L, Pointillart A (2000) The bioavailability of dietary calcium. J Am Coll Nutr
622 19:119S-136S. https://doi.org/10.1080/07315724.2000.10718083
623 9. Allen LH (1982) Calcium bioavailability and absorption: a review. Am J Clin Nutr 35:783–
624 808. https://doi.org/10.1093/ajcn/35.4.783
625 10. Skibsted LH (2016) Mineral nutrient interaction: Improving bioavailability of calcium and
626 iron. Food Sci Biotechnol 25:1233. https://doi.org/10.1007/s10068-016-0196-2
627 11. Rosen CJ, Bouillon R, Compston J, Rosen V (2013) Primer on the metabolic bone diseases
628 and disorders of mineral metabolism, 8th edn. Wiley-Blackwell, Hoboken, NJ.
629 12. Pansu D, Bellaton C, Bronner F (1981) Effect of Ca intake on saturable and nonsaturable
630 components of duodenal Ca transport. Am J Physiol 240:G32–G37.
631 https://doi.org/10.1152/ajpgi.1981.240.1.g32
632 13. Bronner F, Pansu D (1999) Nutritional aspects of calcium absorption. J Nutr 129:9–12.
633 https://doi.org/10.1093/jn/129.1.9
634 14. Moerkens R, Mooiweer J, Smits E, Berg M, Ramírez-Sánchez AD, Modderman R, Puschhof
635 J, Pleguezuelos-Manzano C, Barrett RJ, Wijmenga C, Jonkers IH, Withoff S (2025) Intestine-on-

636 chip enhances nutrient and drug metabolism and maturation of iPSC-derived intestinal epithelial
637 cells relative to organoids and Transwells. Stem Cell Rep 20:102715.
638 https://doi.org/10.1016/j.stemcr.2025.102715
639 15. Zhang D, Qiao L (2023) Intestine-on-a-chip for intestinal disease study and pharmacological
640 research. View 4:20220037. https://doi.org/10.1002/viw.20220037
641 16. Kasendra M, Tovaglieri A, Sontheimer-Phelps A, Jalili-Firoozinezhad S, Bein A,
642 Chalkiadaki A, Scholl W, Zhang C, Rickner H, Richmond CA, Li H, Breault DT, Ingber DE
643 (2018) Development of a primary human Small Intestine-on-a-Chip using biopsy-derived
644 organoids. Sci Rep 8:1–14. https://doi.org/10.1038/s41598-018-21201-7
645 17. Özkan A, LoGrande NT, Feitor JF, Goyal G, Ingber DE (2024) Intestinal organ chips for
646 disease modelling and personalized medicine. Nat Rev Gastroenterol Hepatol 21:751–773.
647 https://doi.org/10.1038/s41575-024-00968-3
648 18. Bein A, Fadel CW, Swenor B, Cao W, Powers RK, Camacho DM, Naziripour A, Parsons A,
649 LoGrande N, Sharma S, Kim S, Jalili-Firoozinezhad S, Grant J, Breault DT, Iqbal J, Ali A,
650 Denson LA, Moore SR, Prantil-Baun R, Goyal G, Ingber DE (2022) Nutritional deficiency in an
651 intestine-on-a-chip recapitulates injury hallmarks associated with environmental enteric
652 dysfunction. Nat Biomed Eng 6:1236–1247. https://doi.org/10.1038/s41551-022-00899-x
653 19. Sontheimer-Phelps A, Chou DB, Tovaglieri A, Ferrante TC, Duckworth T, Fadel C,
654 Frismantas V, Sutherland AD, Jalili-Firoozinezhad S, Kasendra M, Stas E, Weaver JC,
655 Richmond CA, Levy O, Prantil-Baun R, Breault DT, Ingber DE (2020) Human Colon-on-a-Chip
656 Enables Continuous In Vitro Analysis of Colon Mucus Layer Accumulation and Physiology.
657 Cell Mol Gastroenterol Hepatol 9:507–526. https://doi.org/10.1016/j.jcmgh.2019.11.008

20. Garcia-Gutierrez E, Cotter PD (2022) Relevance of organ(s)-on-a-chip systems to the investigation of food-gut microbiota-host interactions. Crit Rev Microbiol 48:463–488. https://doi.org/10.1080/1040841x.2021.1979933

21. Morelli M, Cabezuelo Rodríguez M, Queiroz K (2024) A high-throughput gut-on-chip platform to study the epithelial responses to enterotoxins. Sci Rep 14:1–13. https://doi.org/10.1038/s41598-024-56520-5

22. Ramadan Q, Jafarpoorchekab H, Huang C, Silacci P, Carrara S, Koklü G, Ghaye J, Ramsden J, Ruffert C, Vergeres G, Gijs MAM (2013) NutriChip: nutrition analysis meets microfluidics. Lab Chip 13:196–203. https://doi.org/10.1039/c2lc40845g

23. Feitor JF, Brazaca LC, Lima AM, Ferreira VG, Kassab G, Bagnato VS, Carrilho E, Cardoso DR (2023) Organ-on-a-Chip for Drug Screening: A Bright Future for Sustainability? A Critical Review. ACS Biomater Sci Eng 9:2220–2234. https://doi.org/10.1021/acsbiomaterials.2c01454

24. Ma HL, Urbaczek AC, Souza FZR, Leão PAGGC, Perussi JR, Carrilho E (2021) Rapid Fabrication of Microfluidic Devices for Biological Mimicking: A Survey of Materials and Biocompatibility. Micromachines 12:346. https://doi.org/10.3390/mi12030346

25. Garcia AC, Vavrusova M, Skibsted LH (2018) Supersaturation of calcium citrate as a mechanism behind enhanced availability of calcium phosphates by presence of citrate. Food Res Int 107:195–205. https://doi.org/10.1016/j.foodres.2018.02.020

26. Abcam (n.d.) MTT assay and its use in cell viability and proliferation analysis. https://www.abcam.com/en-us/knowledge-center/cell-biology/mtt-assay. Accessed 9 November 2026.

27. Strober W (2015) Trypan Blue Exclusion Test of Cell Viability. Curr Protoc Immunol 111:A3.B.1-A3.B.3. https://doi.org/10.1002/0471142735.ima03bs111

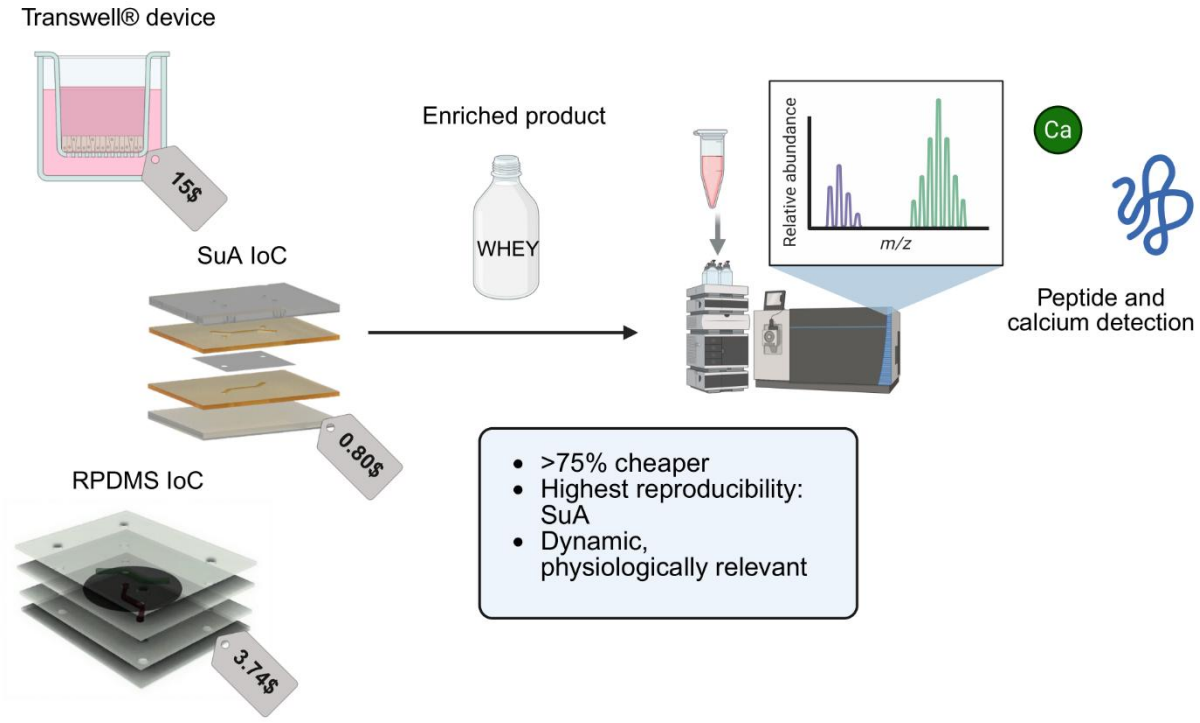
681 28. Thermo Fisher (n.d.) LIVE/DEAD Viability/Cytotoxicity Kit for Mammalian Cells.
682 https://www.thermofisher.com/mx/es/home/references/protocols/cell-and-tissue-
683 analysis/protocols/live-dead-viability-cytotoxicity-kit-for-mammalian-cells.html. Accessed 9
684 November 2026.
685 29. Zhang X, Cheng X, Wu Y, Feng D, Qian Y, Chen L, Yang B, Gu M (2019) In Vitro and In
686 Situ Characterization of the Intestinal Absorption of Capilliposide B and Capilliposide C from
687 Lysimachia capillipes Hemsl. Molecules 24:1227. https://doi.org/10.3390/molecules24071227
688 30. Wu YT, Chen YC (2006) Determination of calcium in complex samples using functional
689 magnetic beads combined with electrodeless/sheathless electrospray ionization mass
690 spectrometry. Rapid Commun Mass Spectrom 20:1995–1999. https://doi.org/10.1002/rcm.2548
691 31. Tang N, Skibsted LH (2016) Calcium Binding to Amino Acids and Small Glycine Peptides
692 in Aqueous Solution: Toward Peptide Design for Better Calcium Bioavailability. J Agric Food
693 Chem 64:4376–4389. https://doi.org/10.1021/acs.jafc.6b01534
694 32. Cross KJ, Huq NL, Palamara JE, Perich JW, Reynolds EC (2005) Physicochemical
695 characterization of casein phosphopeptide-amorphous calcium phosphate nanocomplexes. J Biol
696 Chem 280:15362–15369. https://doi.org/10.1074/jbc.m413504200
697 33. Sato R, Noguchi T, Naito H (1986) Casein phosphopeptide (CPP) enhances calcium
698 absorption from the ligated segment of rat small intestine. J Nutr Sci Vitaminol 32:67–76.
699 https://doi.org/10.3177/jnsv.32.67
700 34. Thomä C, Krause I, Kulozik U (2006) Precipitation behaviour of caseinomacropeptides and
701 their simultaneous determination with whey proteins by RP-HPLC. Int Dairy J 16:285–293.
702 https://doi.org/10.1016/j.idairyj.2005.05.003

703 35. Malkoski M, Dashper SG, O'Brien-Simpson NM, Talbo GH, Macris M, Cross KJ, Reynolds
704 EC (2001) Kappacin, a novel antibacterial peptide from bovine milk. Antimicrob Agents
705 Chemother 45:2309–2315. https://doi.org/10.1128/aac.45.8.2309-2315.2001
706 36. Talbo GH, Suckau D, Malkoski M, Reynolds EC (2001) MALDI-PSD-MS analysis of the
707 phosphorylation sites of caseinomacropeptide. Peptides 22:1093–1098.
708 https://doi.org/10.1016/s0196-9781(01)00426-0
709 37. Petrat-Melin B, Le TT, Møller HS, Larsen LB, Young JF (2017) Short communication:
710 Inhibition of angiotensin 1-converting enzyme by peptides derived from variants of bovine β-
711 casein upon apical exposure to a Caco-2 cell monolayer. J Dairy Sci 100:881–885.
712 https://doi.org/10.3168/jds.2016-11684
713 38. Jobst KJ, Terlouw JK, Luider TM, Burgers PC (2008) On the interaction of peptides with
714 calcium ions as studied by matrix-assisted laser desorption/ionization Fourier transform mass
715 spectrometry: towards peptide fishing using metal ion baits. Anal Chim Acta 627:136–147.
716 https://doi.org/10.1016/j.aca.2008.03.028
717 39. Wang L, Klopot A, Freund JN, Dowling LN, Krasinski SD, Fleet JC (2004) Control of
718 differentiation-induced calbindin-D9k gene expression in Caco-2 cells by cdx-2 and HNF-1α.
719 Am J Physiol Gastrointest Liver Physiol 287:G943–G953.
720 https://doi.org/10.1152/ajpgi.00121.2004
721 40. Taparia S, Fleet JC, Peng JB, Wang XD, Wood RJ (2006) 1,25-Dihydroxyvitamin D and 25-
722 hydroxyvitamin D–mediated regulation of TRPV6 (a putative epithelial calcium channel) mRNA
723 expression in Caco-2 cells. Eur J Nutr 45:196–204. https://doi.org/10.1007/s00394-005-0586-3
724 41. Brodkorb A, Egger L, Alminger M, Alvito P, Assunção R, Ballance S, Bohn T, Bourlieu-
725 Lacanal C, Boutrou R, Carrière F, Clemente A, Corredig M, Dupont D, Dufour C, Edwards C,

Golding M, Karakaya S, Kirkhus B, Le Feunteun S, Lesmes U, Macierzanka A, Mackie AR, Martins C, Marze S, McClements DJ, Ménard O, Minekus M, Portmann R, Santos CN, Souchon I, Singh RP, Vegarud GE, Wickham MSJ, Weitschies W, Recio I (2019) INFOGEST static in vitro simulation of gastrointestinal food digestion. Nat Protoc 14:991–1014. https://doi.org/10.1038/s41596-018-0119-1

42. Corrochano AR, Ferraretto A, Arranz E, Stuknytė M, Bottani M, O'Connor PM, Kelly PM, De Noni I, Buckin V, Giblin L (2019) Bovine whey peptides transit the intestinal barrier to reduce oxidative stress in muscle cells. Food Chem 288:306–314. https://doi.org/10.1016/j.foodchem.2019.03.009

43. Pereira C, Costa J, Sarmento B, Araújo F (2016) Cell-based in vitro models for intestinal permeability studies. In: Concepts and models for drug permeability studies. Elsevier, Amsterdam, pp 57–81. https://doi.org/10.1016/B978-0-08-100094-6.00005-5


Transwell® device
15$
SuA IoC
0.80$
RPDMS IoC
3.74$
Enriched product
WHEY
Relative abundance
m/z
Ca
Peptide and calcium detection
>75% cheaper
Highest reproducibility: SuA
Dynamic, physiologically relevant

741

## Supplementary Files

This is a list of supplementary files associated with this preprint. Click to download.

- FeitorJFEFRTOnlineResourcescorrected.docx